Z. Phys. C – Particles and Fields 51, 557–564 (1991)

Zeitschrift für Physik C Particles and Fields
© Springer-Verlag 1991

Electron-state bremsstrahlung processes $ep \to \gamma ep(X)$ at HERA

A.A. Akhundov[1], D.Yu. Bardin[2], L.V. Kalinovskaja[3]

[1] Institute of Physics, Academy of Sciences of the Azerbaijan, pr. Narimanova 33, SU-370143 Baku, USSR
[2] Joint Institute for Nuclear Research, Dubna, Head Post Office P.O. Box 79, SU-101000 Moscow, USSR
[3] Gomel Polytechnical Institute, SU-246047 Gomel, USSR

Received 29 October 1990

Abstract. The analytic formulae for the bremsstrahlung photon spectra in the processes $lN \to \gamma lN$ and $lN \to \gamma lX$ (taking into account γ- and Z-boson exchange diagrams) are derived. The energy and angular distributions of photons are computed at HERA energies. The very large sensitivity of spectra for the deep inelastic channel to the choice of the structure functions is revealed in the region of small angles and large energies of the emitted photons.

1 Introduction

In connection with forthcoming experiments at the electron–proton collider HERA it is timely to carry out a new and more complete study of electron bremsstrahlung processes in colliding ep- beams. In the framework of QED, bremsstrahlung processes for fixed targets and in colliding $e^{\pm}e^{-}$-beams were carefully studied in the literature and analytic formulae for the cross sections of these processes have been obtained (see, for example, reviews [1, 2]).

Now, the processes $ep \to \gamma ep(X)$ at colliding $e^{\pm}p$-beams are of interest first of all from the point of view of the luminosity measurement in electron–proton colliders [3]. So, the influence of the transverse beam size on the cross section for the QED process $ep \to \gamma ep$ at HERA was studied in [4]. Many distributions for the above process in different kinematical variables have been calculated by a Monte–Carlo method for phase space integration in [5].

The bremsstrahlung processes of the colliding ep-beams are also of interest with regard to the verification of the QED prediction for the radiative corrections. It is well known that radiative corrections to the deep inelastic scattering processes $ep \to e(\nu_e)X$ are of the order of several dozens of percent [6, 7]. Therefore it would be desirable to check the theoretical calculations by measuring the radiative corrections before one starts the analysis of experimental data on deep inelastic scattering at HERA. These checks may be realized as it was done in the muon fixed target experiments at the SPS [8] by comparison of the theoretical photon distributions with the experimental ones.

In the previous paper [7] we have calculated the contribution of the radiative tail from the elastic peak $ep \to e\gamma p$ to the measured cross section $\mathrm{d}^2\sigma/\mathrm{d}x\mathrm{d}y$ in deep inelastic $ep \to eX$ scattering (where x, y are the usual scaling variables of the scattered lepton). In the present note we give the analytic formulae for energy and angular distributions of photons emitted from leptons in the elastic process:

$$l + N \to \gamma + l + N \tag{1}$$

and in the inelastic one

$$l + N \to \gamma + l + N. \tag{2}$$

For the first time formulae are obtained in a general form taking into account both γ-quanta and Z-boson exchange (generalized form factors [7] and structure functions are used), they are valid in the whole kinematical region of the processes (1) and (2). Naturally, a ultrarelativistic approximation is used here $m^2 \ll E_l^2$ (m being the mass and E_l the energy of the initial lepton).

In the experiment H1 it is planned to have a γ-counter which would register photons with energy $1 \leqq E_\gamma \leqq 30\,\mathrm{GeV}$ and emission angle $0 \leqq \theta_\gamma \leqq 0.5\,\mathrm{mrad}$ in the HERA lab. system [9]. Consequently, one of the first purposes of this paper is to calculate these distributions numerically in the practical kinematic region of small angles and large energies of photons.

Our main task is to calculate carefully the inelastic process (2) in the above kinematical range. Of course, we have also calculated the elastic process (1), but the dominant contribution of diagrams with γ-quanta exchange was already studied exhaustively before, [5].*

This paper is organized as follows. In Sect. 2 we define the kinematic variables and kinematic region. In Sect. 3 we give all basic formulae for the contributions of the processes under consideration. Section 4 contains the results and the discussion.

* In this case our results practically agree with those presented in [5]

2 Kinematics

For the description of the elastic reaction (1) we choose five independent invariants:

$$S = -2p_1k_1, \quad X = -2p_1k, \quad Y = -2k_1k,$$
$$t = (p_2 - p_1)^2, \quad z = -2k_2k. \tag{3}$$

In the inelastic case (2), it is convenient to get also the invariant hadron mass:

$$M_X^2 = -p_2^2 \tag{4}$$

or the linearly dependent variable

$$T = t + M_X^2 - M^2 \tag{5}$$

with M being the nucleon mass.

In the following we use some λ-functions written in terms of these invariants:

$$\lambda_S = S^2 - 4m^2M^2,$$
$$\lambda_Y = S_X^2 + 4M^2Y,$$
$$\lambda_K = (W^2 - M_X^2 - m^2)^2 - 4m^2M_X^2$$

where

$$W^2 = M^2 + m^2 + S_X - Y \tag{6}$$

is the invariant mass of the undetected system of particles (electron + hadronic jet) and $S_X = S - X$.

In terms of chosen variables (3) and (4) the phase space takes the form

$$\Gamma = \frac{\pi}{4\sqrt{\lambda_S}} \int \mathrm{d}X\,\mathrm{d}Y\,\mathrm{d}M_X^2 \frac{\mathrm{d}t\,\mathrm{d}z}{\sqrt{R_Z}}, \tag{7}$$

and R_Z denotes the Gram determinant:

$$R_Z = A_Z \cdot z^2 + 2B_Z \cdot z - C_Z,$$
$$A_Z = -\lambda_Y,$$
$$B_Z = 2M^2Y(Y - 2m^2 - t) + X(S_Xt - T(Y - 2m^2)) + SY(S_X - T),$$
$$C_Z = [Xt - Y(S - T)]^2 + 4m^2[X(Xt + YT) - M^2Y^2].$$

One can easily derive the physical region of variation of z and t:

$$z_{\min,\max} = \frac{-B_Z \pm (B_Z^2 + A_ZC_Z)^{1/2}}{A_Z}, \tag{8}$$

$$t_{\max,\min} = Y - 2m^2 + \frac{1}{2W^2}[(W^2 - Y + m^2 - M^2) \cdot (W^2 + m^2 - M_X^2) \pm \sqrt{\lambda_Y}\sqrt{\lambda_K}]. \tag{9}$$

The limits of M_X^2 are given by:

$$M^2 \leqq M_X^2 \leqq (\sqrt{W^2} - m)^2. \tag{10}$$

The kinematics of the elastic case (1) follows from the general kinematics of the inelastic process (2) if $M_X^2 = M^2$.

The variables S, X and Y define the energy E_γ and the emission angle θ_γ of photons in the laboratory system:

$$S = 2E_lE_N(1 + \beta_l\beta_N), \tag{11}$$

$$X = 2E_\gamma E_N(1 + \beta_N \cos\theta_\gamma), \tag{12}$$

$$Y = 2E_\gamma E_l(1 - \beta_l \cos\theta_\gamma), \tag{13}$$

where E_N is the energy of the incoming nucleon and

$$\beta_l = \left(1 - \frac{m^2}{E_l^2}\right)^{1/2}, \quad \beta_N = \left(1 - \frac{M^2}{E_N^2}\right)^{1/2}. \tag{14}$$

The physical region of E_γ and θ_γ reads as follows:

$$0 \leqq \theta_\gamma \leqq \pi, \tag{15}$$

$$0 \leqq \frac{E_\gamma}{E_l} \leqq \frac{1 + \beta_l\beta_N - \frac{m}{E_l}\frac{M}{E_N}}{1 + \beta_N \cos\theta_\gamma + \frac{E_l}{E_N}(1 - \beta_l \cos\theta_\gamma)}. \tag{16}$$

3 Inclusive cross section

For the description of the deep inelastic interaction of unpolarized nucleons with γ-quanta or Z-bosons we have to use the phenomenological hadron tensor:

$$W_{\mu\nu} = \sum_{a=\gamma,I,Z} W_{\mu\nu}^a, \tag{17}$$

$$W_{\mu\nu}^a = W_1^a\left(\delta_{\mu\nu} - \frac{q_\mu q_\nu}{q^2}\right) + \frac{W_2^a}{M^2}\left(p_{1\mu} - \frac{p_1q}{q^2}q_\mu\right) \cdot \left(p_{1\nu} - \frac{p_1q}{q^2}q_\nu\right) + \frac{W_3^a}{2M^2}e_{\mu\nu\rho\sigma}p_{1\rho}q_\sigma, \tag{18}$$

where $W_i^a (a = \gamma, I, Z; i = 1, 2, 3)$ are real functions of the invariants q^2 and p_1q.

In the ultrarelativistic approximation the following combinations of W_i^a enter the cross section of the scattering off unpolarized nucleons:

$$(2MW_1)^{\mathrm{gen}} \equiv (2MW_1)^\gamma + 2\chi|Q_l|v_l(2MW_1)^I + \chi^2(v_l^2 + a_l^2)(2MW_1)^Z, \tag{19}$$

$$\left(\frac{W_2}{2M}\right)^{\mathrm{gen}} \equiv \left(\frac{W_2}{2M}\right)^\gamma + 2\chi|Q_l|v_1\left(\frac{W_2}{2M}\right)^I + \chi^2(v_l^2 + a_l^2)\left(\frac{W_2}{2M}\right)^Z, \tag{20}$$

$$\left(\frac{W_3}{4M}\right)^{\mathrm{gen}} \equiv 2\chi(-Q_l)a_l\left(\frac{W_3}{4M}\right)^I + 2\chi^2(-Q_l)v_la_l\left(\frac{W_3}{4M}\right)^Z. \tag{21}$$

Here v_l and a_l are the vector and axial coupling constants of the lepton with Z-boson:

$$v_l = 1 - 4|Q_l|\sin^2\theta_w, \quad a_l = 1, \tag{22}$$

(θ_w is the weak mixing angle, Q_l is the lepton charge, $Q_e = -1$)

$$\chi = \frac{G_\mu}{\sqrt{2}}\frac{M_Z^2}{8\pi\alpha}\frac{t}{t + M_Z^2}, \tag{23}$$

G_μ is the Fermi constant: $G_\mu = 1.16637 \cdot 10^{-5}\,\mathrm{GeV}^{-2}$.

These generalized structure functions (19–21), describing the electroweak interaction of γ, Z-bosons with

unpolarized nucleons may be written as:

$$A_1(T,t) \equiv (2MW_1)^{\text{gen}} = 2[F_1(T,t) + 2\chi|Q_l|v_l G_1(T,t) + \chi^2(v_l^2 + a_l^2)H_1(T,t)], \quad (24)$$

$$A_2(T,t) \equiv \frac{1}{T}(\nu W_2)^{\text{gen}} = \frac{1}{T}[F_2(T,t) + 2\chi|Q_l|v_l G_2(T,t) + \chi^2(v_l^2 + a_l^2)H_2(T,t)], \quad (25)$$

$$A_3(T,t) \equiv \frac{1}{2T}(\nu W)^{\text{gen}} = \frac{1}{2T}[2\chi(-Q_l)a_l(G_3(T,t) + \chi v_l H_3(T,t))]. \quad (26)$$

The relation of the generalized structure functions $A_i(T,t)(i=1,2,3)$ with the generalized elastic form factors $A_i(t)(i=1,2,3)$ (they describe elastic interactions of γ, Z-bosons with the nonpolarized nucleons) follows from (19–21):

$$A_1(T,t) = tA_1(t)\delta(T-t), \quad (27)$$

$$A_2(T,t) = A_2(t)\delta(T-t), \quad (28)$$

$$A_3(T,t) = A_3(t)\delta(T-t), \quad (29)$$

where $A_i(t)$ are determined by formulae (20–22) of [7]. By this, the hadron vertex in the elastic case (1) is expressed in terms of model-independent generalized form factors $A_i(t)$. Their calculation is carefully described in [7].

The differential cross section of the unpolarized particle scattering corresponding to the diagrams of Fig. 1 can be written in the ultrarelativistic approximation as

$$d\sigma = \frac{2\sigma^3}{\pi S^2} S(T,t,z)\,dX\,dY\frac{dM_X^2\,dt\,dz}{t^2(R_Z)^{1/2}}, \quad (30)$$

$$S(T,t,z) = A_1(T,t)S_1(T,t,z) + A_2(T,t)S_2(T,t,z) + A_3(T,t)S_3(T,t,z), \quad (31)$$

where three factorized functions $S_1(T,t,z)$, $S_2(T,t,z)$ and $S_3(T,t,z)$ are explicitly calculated expressions:

$$S_1(T,t,z) = (t-2m^2)\left[-m^2\left(\frac{1}{z^2}+\frac{1}{Y^2}\right) + (t+2m^2)\frac{1}{zY} - \frac{1}{z} + \frac{1}{Y}\right] + \frac{1}{2}\left(\frac{Y}{z}+\frac{z}{Y}\right), \quad (32)$$

$$S_2(T,t,z) = -2m^2\left[\frac{1}{z^2}(S(S-T)-M^2t) + \frac{1}{Y^2}(S_X(S_X-T)-M^2t)\right] - \frac{1}{z}(T(S_X-T)-2M^2t) - \frac{1}{Y}(TS+2M^2t) + \frac{1}{zY}[t(S^2+S_X^2-2M^2t) - T(S+S_X)(t+2m^2) + 4m^2(SS_X-M^2t)] - M^2\left(\frac{Y}{z}+\frac{z}{Y}\right), \quad (33)$$

$$S_3(T,t,z) = -2m^2\left[\frac{1}{z^2}(2S-T) + \frac{1}{Y^2}(2S_X-T)\right] - 2t\left(\frac{S_X}{z} - \frac{S-T}{Y}\right) + \frac{2}{zY}[t^2(S-T+S_X) + 2m^2(t(S-T)+TS_X)] + T\left(\frac{Y}{z}-\frac{z}{Y}\right). \quad (34)$$

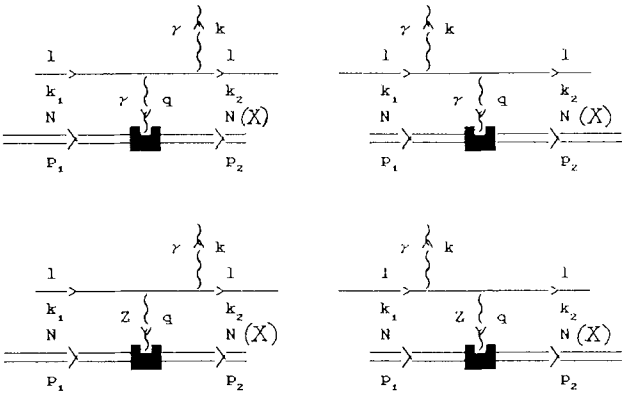

Fig. 1. Feynman graphs corresponding to the processes considered in this paper

Integrating $S(M_X^2,t,z)$ over the invariant z within the limits (8), we derive the following expression:

$$S(T,t) \equiv \frac{1}{\pi}\int \frac{dz}{t^2\sqrt{R_Z}} S(M_X^2,t,z) = A_1(T,t)S_1(T,t) + A_2(T,t)S_2(T,t) + A_3(T,t)S_3(T,t), \quad (35)$$

where $S_i(T,t)$ are

$$S_1(T,t) = \frac{1}{(C_Z)^{1/2}}\left[\frac{1}{Y} - \frac{1}{t} + \frac{1}{t^2}\left(\frac{Y}{2} + 2m^2\left(1-\frac{2m^2}{Y}\right)\right)\right] + m^2\frac{B_Z}{t(C_Z)^{3/2}}\left(\frac{2m^2}{t}-1\right) + \frac{1}{tY\sqrt{\lambda_Y}}\left[\frac{B_Z}{2t\lambda_Y} + \left(\frac{m^2}{Y}-1\right)\left(\frac{2m^2}{t}-1\right)\right], \quad (36)$$

$$S_2(T,t) = \frac{1}{(C_Z)^{1/2}}\left[2M^2\left(\frac{1}{t}-\frac{1}{Y}-\frac{2m^2}{tY}+\frac{Y}{2t^2}\right) + \frac{1}{tY}\left(S^2+S_X^2 - T(S+S_X)\left(1+\frac{2m^2}{t}\right) + \frac{4m^2}{t}SS_X\right) - \frac{T}{t^2}(S_X-T)\right] + 2m^2\frac{B_Z}{t^2(C_Z)^{3/2}}[M^2t - S(S-t)]$$

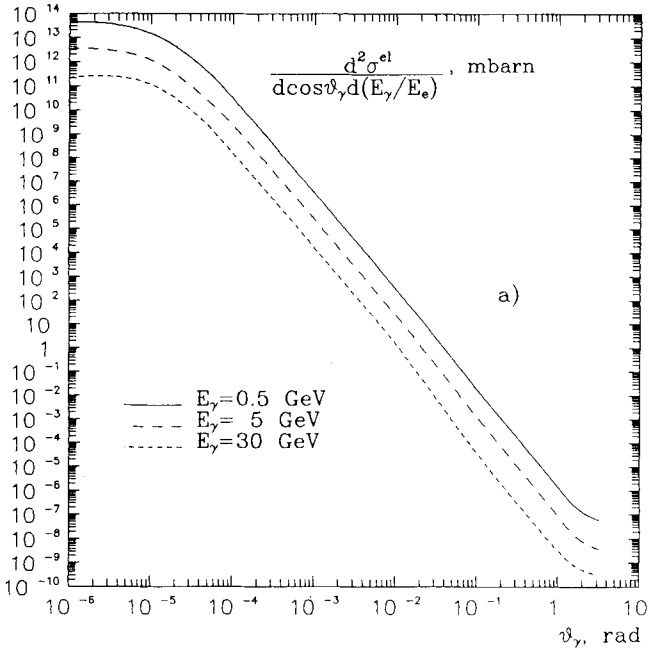

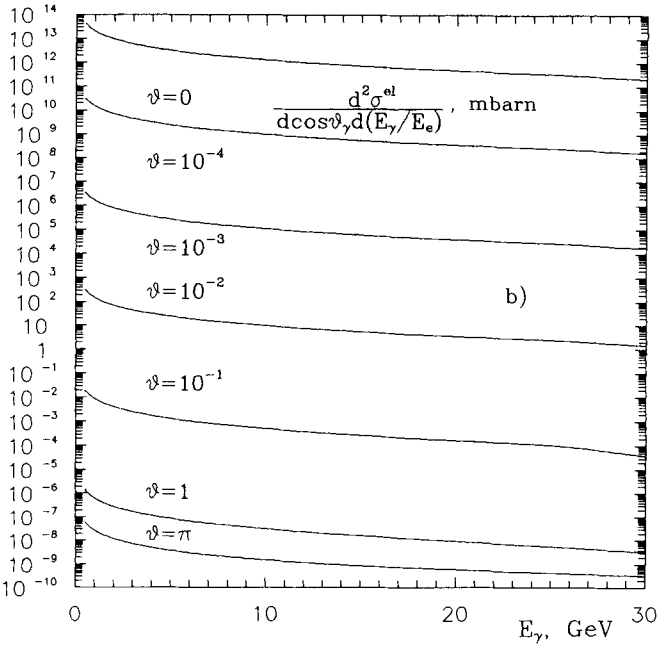

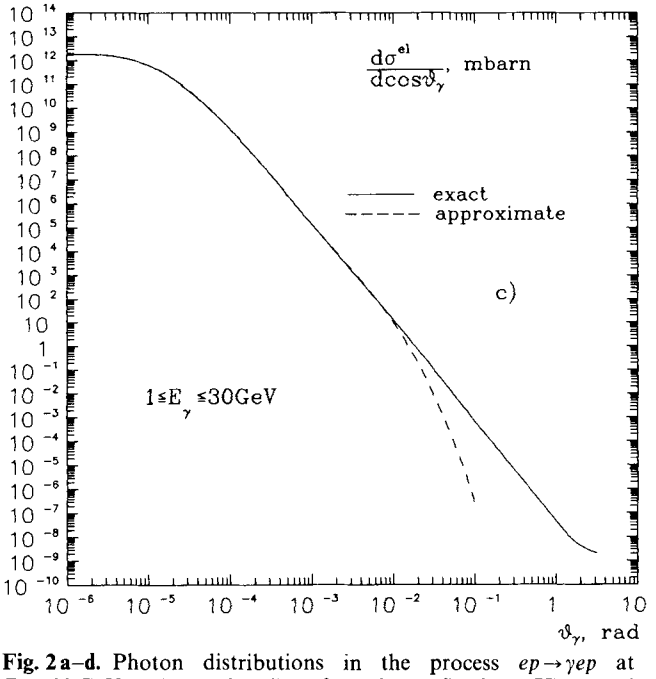

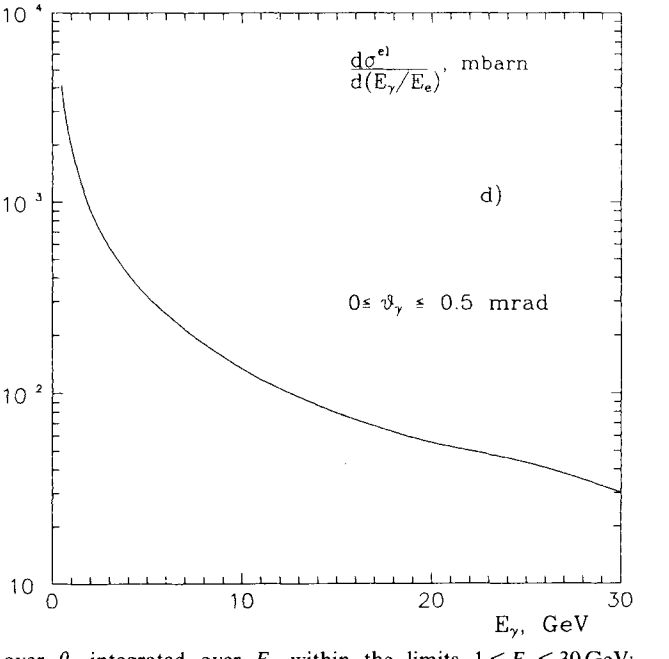

Fig. 2a–d. Photon distributions in the process $ep \to \gamma ep$ at $E_e = 30\,\text{GeV}$ and $E_p = 820\,\text{GeV}$; form factor fits from [7]: **a** and **b** double differential cross-sections in θ_γ and E_γ; **c** distribution over θ_γ integrated over E_γ within the limits $1 \leqq E_\gamma \leqq 30\,\text{GeV}$; **d** distribution over E_γ integrated over θ_γ within the limits $0 \leqq \theta_\gamma \leqq 0.5\,\text{mrad}$

$$+\frac{1}{tY\sqrt{\lambda_Y}}\left[2M^2\left(-\frac{B_Z}{2t\lambda_Y}+\frac{m^2}{Y}-1\right)\right.$$
$$\left.-\frac{1}{t}\left(ST+\frac{2m^2}{Y}S_X(S_X-T)\right)\right], \tag{37}$$

$$S_3(T,t)=\frac{1}{(C_Z)^{1/2}}\left[\frac{2}{Y}(S+S_X-T)\left(1+\frac{2m^2}{t}\right)\right.$$
$$\left.-\frac{2S_X}{t}+\frac{YT}{t^2}\right]-2m^2\frac{B_Z}{t(C_Z)^{3/2}}(2S-T)$$
$$+\frac{2}{tY\sqrt{\lambda_Y}}\left[-\frac{B_ZT}{2t\lambda_Y}+S-T-\frac{m^2}{Y}(2S_X-T)\right]. \tag{38}$$

These covariant formulae may be used for the calculation of the various distributions of photon bremsstrahlung characteristics in the reactions (1) and (2). The formulae of the elastic process (1) follow from the general formulae of reaction (2), if we use the relations (27–29).

So, the double-differential cross section over the emission angle θ_γ and the energy E_γ of a photon in the lab. system is:

$$\frac{d^2\sigma^{inel}}{d\cos\theta_\gamma d(E_\gamma/E_N)} = \frac{2\alpha^3 E_\gamma}{E_N(1+\beta_N)} \int dM_X^2 \int dt S(T,t). \quad (39)$$

4 Discussion of results

We have calculated the energy and angular distributions of bremsstrahlung photons in the processes:

$$e + p \to \gamma + e + p, \quad (40)$$

$$e + p \to \gamma + e + X, \quad (41)$$

with $E_e = 30\,\text{GeV}$ and $E_p = 820\,\text{GeV}$.

The results for the reaction (40), presented in Fig. 2 are in complete agreement with those from [5]; they will serve us as a reference of the comparison with the new results obtained for the process (41). When calculating the cross-sections of the process (40) we have taken the same fit for the elastic form factors of the proton as in [7].

In Fig. 2c we presented numerical results derived with the aid of an approximate formula which does not contain

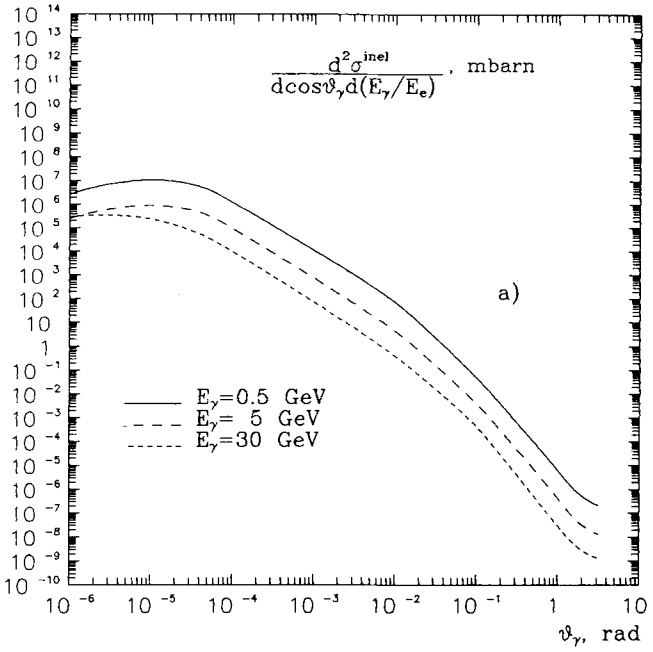

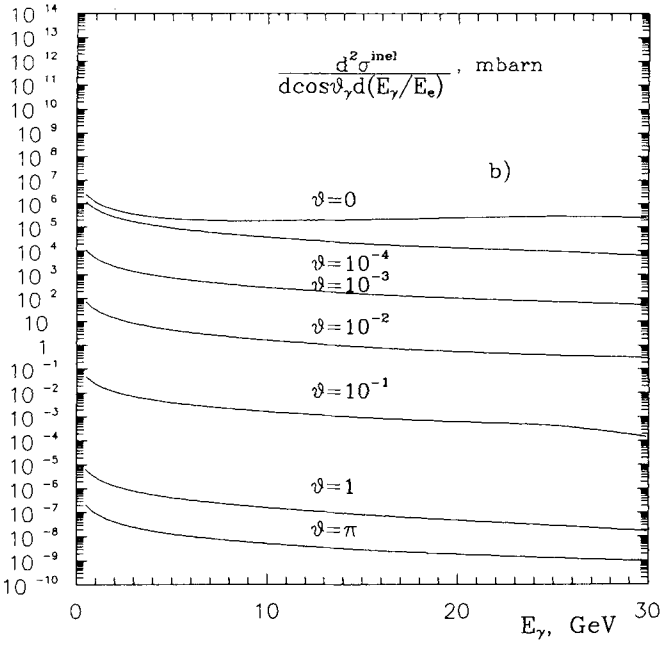

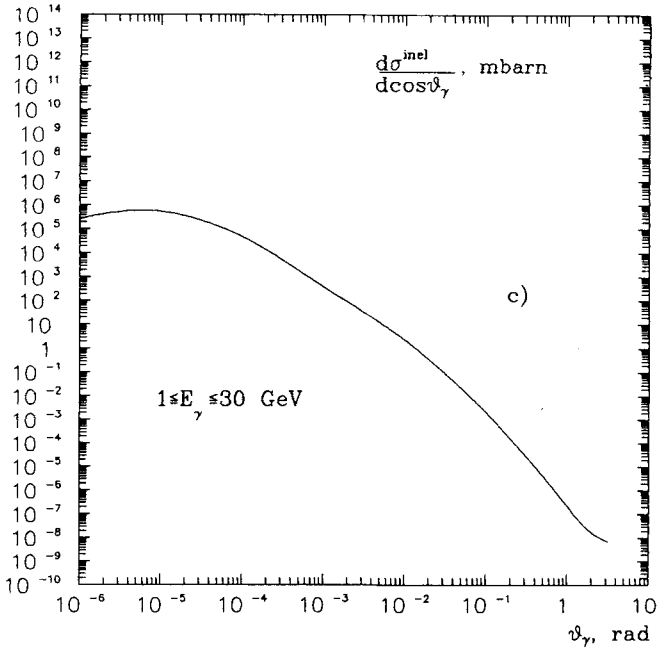

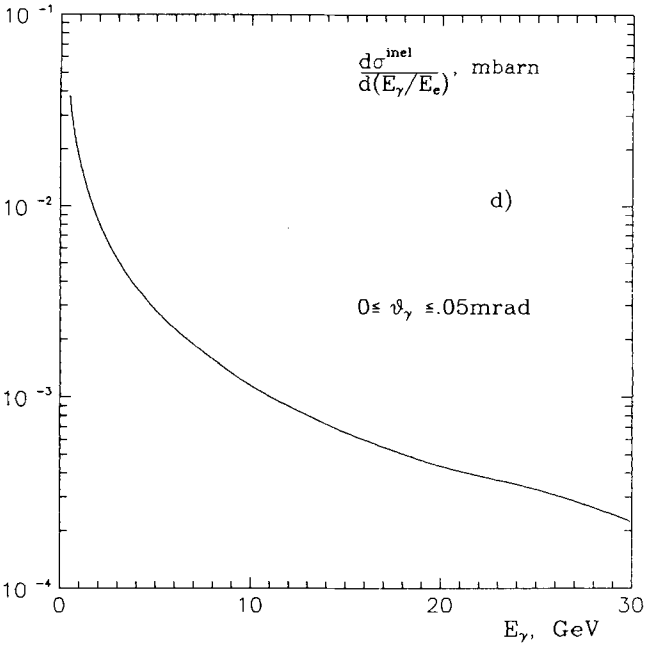

Fig. 3a–d. Photon distributions in the process $ep \to \gamma eX$ at $E_e = 30\,\text{GeV}$ and $E_p = 820\,\text{GeV}$; structure function fits from [10, 11, 13]: **a** and **b** double differential cross-sections in θ_γ and E_γ: **c** distribution over θ_γ integrated over E_γ within the limits $1 \leqq E_\gamma \leqq 30\,\text{GeV}$; **d** distribution over E_γ integrated over θ_γ within the limits $0 \leqq \theta_\gamma \leqq 0.5\,\text{mrad}$

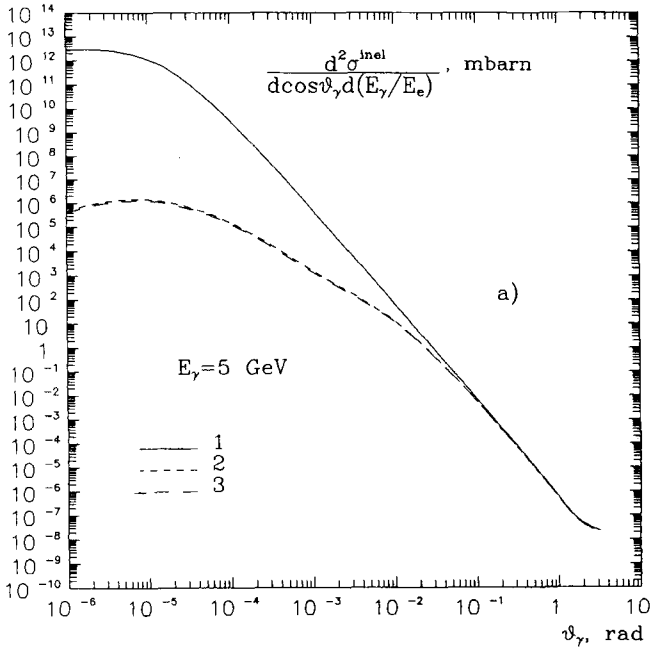

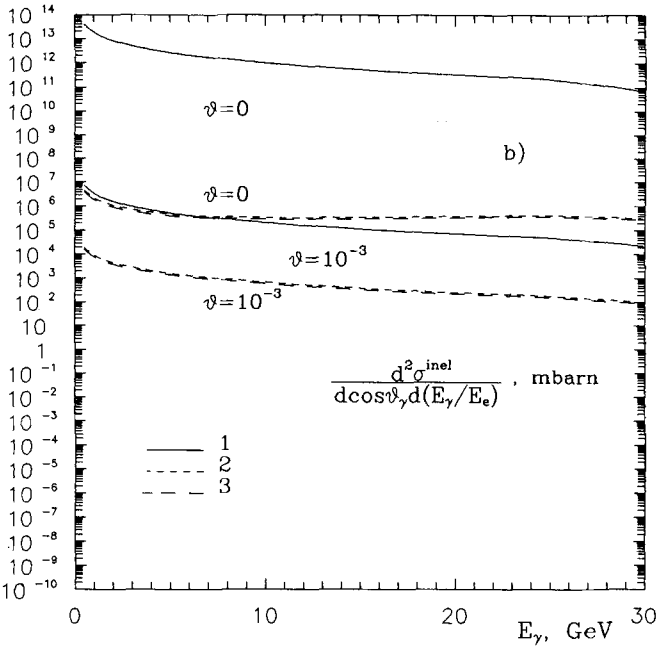

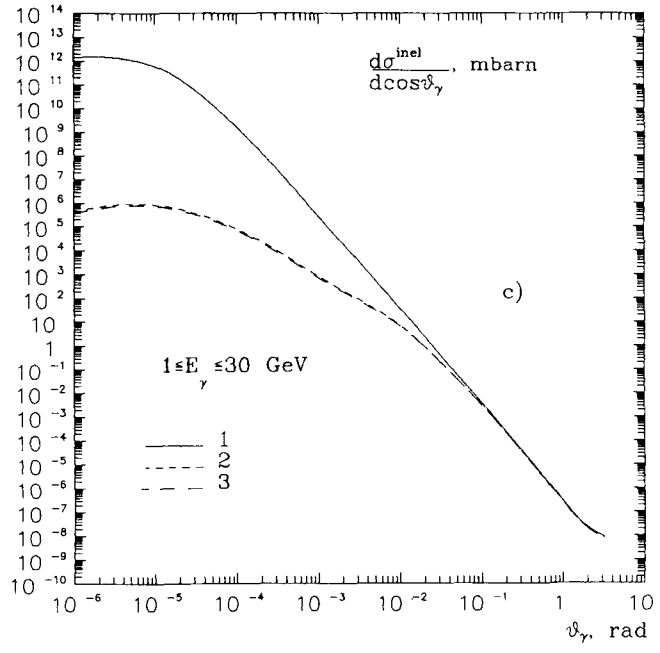

Fig. 4a–c. Photon distributions in the process $ep \to \gamma eX$ at $E_e = 30\,\text{GeV}$ and $E_p = 820\,\text{GeV}$: **a** and **b** double differential cross-sections in θ_γ and E_γ; **c** distribution over θ_γ integrated over E_γ within the limits $1 \leqq E_\gamma \leqq 30\,\text{GeV}$. The numbers near the curves specify the structure function fits used in the full phase space (regions 1, 2 and 3): 1 the structure functions fit from [13], 2 and 3 to the "corrected" structure functions (51) and (52), respectively

any integration as in (39). The approximation is based on the assumption that most of the bremsstrahlung photons are emitted collinearly to the incoming and outgoing electrons. As it is seen, this approximation is valid at small angles ($\theta_\gamma \leqq 10\,\text{mrad}$) but not at large θ_γ.

For the elastic process we calculated also the total cross-section

$$\sigma(ep \to \gamma ep) = 173.6 \cdot 10^{-27}\,\text{cm}^2, \tag{42}$$

corresponding to the integration over the angle and the energy within the limits:

$$0 \leqq \theta_\gamma \leqq 0.5\,\text{mrad}, \quad 1 \leqq E_\gamma \leqq 30\,\text{GeV}. \tag{43}$$

For the following discussion one needs to specify which structure functions were used for the calculation of deep inelastic reactions (41) (see Figs. 3, 4).

For the calculation of the inclusive cross-section of the process at some point (Y, W^2) of the kinematic region one needs to know the generalized structure functions $A_i(M_X^2, t)$ within the triangle CDF (Fig. 5). The dominant contribution to the cross-section of the deep inelastic reaction (41), as in the case of the elastic one (40), comes from diagrams with γ-exchange. The other contributions (γZ) and (ZZ) are less than two percent for $\theta_\gamma \leqq 1\,\text{rad}$, reaching dozens of percent only in the vicinity of $\theta_\gamma = \pi$. That is why it is very important to make a correct choice

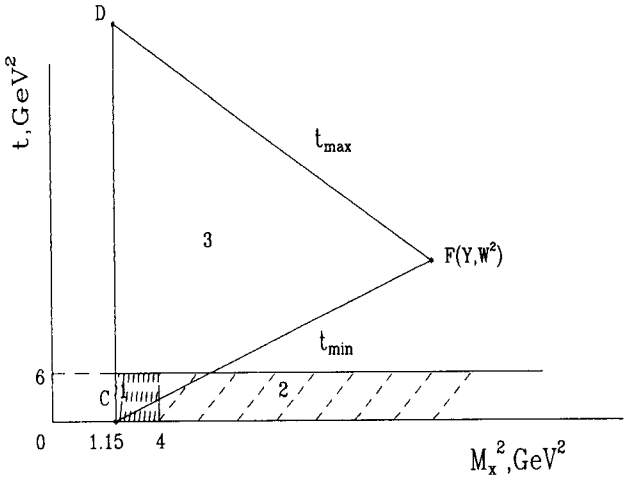

Fig. 5. The kinematical region of the deep inelastic process in the (M_X^2, t)-plane

of the structure functions $F_1(M_X^2, t)$ and $F_2(M_X^2, t)$ which are well investigated in a wide region of variation of the kinematical variables M_X^2 and t. Moreover, since the main contribution to the cross-section comes from the region of small t, it is important to use realistic fits of the structure functions F_1 and F_2 in this region instead of quark–parton model parametrizations which are bound to fail here.

Such fits in our view are the fits from papers by Brasse et al. [10], (region 1 in Fig. 5) and by Stein et al. [11] (region 2 in Fig. 5), which are obtained by means of the model-independent analysis of deep inelastic ep-scattering at low energies ($E \leqq 20\,\text{GeV}$). These fits have the correct behaviour at $t \to 0$, namely:

$$F_2(M_X^2, t) = ct. \tag{44}$$

The fit from [10] is valid only in the region 1 (Fig. 5), and the fit from [11] may be extrapolated to the whole region 2 of Fig. 5 although it was obtained in the region $4 \leqq M_X^2 \leqq 25\,\text{GeV}^2$ and $0 \leqq t \leqq 2\,\text{GeV}^2$, see [12].

In the rest region 3 ($t > 6\,\text{GeV}^2$) for $F_{1,2}$ and also for $G_{1,2,3}$ and $H_{1,2,3}$ in all regions we have used the structure functions expressed through the quark distributions $f_q(x, Q^2)$ and $\bar{f}_q(x, Q^2)$:

$$F_2(x, Q^2) = 2xF_1(x, Q^2) = x\sum_q e_q^2[f_q(x, Q^2) + \bar{f}_q(x, Q^2)], \tag{45}$$

$$G_2(x, Q^2) = 2xG_1(x, Q^2) = x\sum_q |e_q| v_q[f_q(x, Q^2) + \bar{f}_q(x, Q^2)], \tag{46}$$

$$G_3(x, Q^2) = \sum_q |e_q| a_q[f_q(x, Q^2) - \bar{f}_q(x, Q^2)], \tag{47}$$

$$H_2(x, Q^2) = 2xH_1(x, Q^2) = x\sum_q (v_q^2 + a_q^2)[f_q(x, Q^2) + \bar{f}_q(x, Q^2)], \tag{48}$$

$$H_3(x, Q^2) = 2\sum_q v_q a_q[f_q(x, Q^2) - \bar{f}_q(x, Q^2)]. \tag{49}$$

Here Q^2 is the momentum transfer squared, x is the scaling variable, e_q is the quark charge, and v_q and a_q are the vector and axial quark couplings to the Z-boson,

$$v_q = 1 - 4|e_q| \cdot \sin^2 \theta_w, \quad a_q = 1. \tag{50}$$

The results for the photon spectra in process (41) are presented in Fig. 3. They are obtained with the fits of the structure functions F_1, F_2 from [10, 11] in the regions 1 and 2, respectively, and of F_i, G_i and H_i given by (45–49) with quark distributions taken from the paper of Duke and Owens [13].

From a comparison of Fig. 2 and Fig. 3 it is seen that the general behaviour of the photon spectra in the elastic and inelastic processes are similar for the E_γ distribution but not for θ_γ. The average emission angle of photons in the inelastic case is about 2 orders of magnitude larger than in the elastic one. This is an apparent consequence of the different behaviour of the structure function $F_2(M_X^2, t)$ and its elastic analog $W_2^{\text{el}}(t)$ when $t \to 0$; while the first vanishes, the second goes to a constant. The absolute cross-section for the process (41) is about 7 orders of magnitude lower as compared to the cross section of the process (40).

The sensitivity of the spectra for the inelastic reaction (41) to the choice of the structure functions is illustrated in Fig. 4, where we calculated also photonic distributions with two variants of "corrected" structure functions:

$$A_i(M_X^2, t) \to A_i(M_X^2, t)(1 - W_2^{\text{el}}(t)), \tag{51}$$

or

$$A_i(M_X^2, t) \to A_i(M_X^2, t)(1 - \exp(-a^2 t)), \tag{52}$$

where

$$W_2^{\text{el}}(t) = \frac{G_e^2 + \tau G_m^2}{1 + \tau}, \quad \tau = \frac{t}{4M^2} \tag{53}$$

and $a^2 = 3.37\,\text{GeV}^{-2}$. These corrections were introduced in [11, 14] correspondingly; they are motivated to a great extent by (44).

As it is seen from Figs. 3, 4 the use of the standard parton–model formulae with a fit for $f_q(x, Q^2)$ and $\bar{f}_q(x, Q^2)$ leads to an overestimation of the result in the region of small θ_γ and large E_γ by 6–7 orders of magnitude as compared to the results derived with the realistic structure functions, as in Fig. 3.

The last observation has a very important consequences. The region of small θ_γ and large E_γ corresponds to the region of small x and large y, where radiative corrections are very large ($\sim 100\%$) (see e.g. [6]). But almost all previous calculations of the radiative corrections at HERA energies were based on the parameterizations of the structure functions through quark distributions. Apparently the realistic structure functions satisfying the requirement (44) decrease the value of the radiative corrections at small x. This conclusion is in agreement with the early observed correction behaviour in [12] and is the reason why in [6] radiative corrections were not presented for x less than 0.01. The more detailed investigation of this problem composes the subject of a separate publication.

Acknowledgements. The authors are very much obliged to M. Klein, W. Krasny, W. von Schlippe and H. Spiesberger for useful discussions and the critical reading of manuscript. We are very much obliged to G. Kramer for useful suggestions and support.

References

1. L.W. Mo, Y.S. Tsai: Rev. Mod. Phys. 41 (1969) 205
2. V.N. Baier, V.S. Fadin, V.A. Khoze, E.A. Kuraev: Phys. Rep. C78 (1981) 293
3. D. Barber et al.: Proc. XIII Int. Conf. on High Energy Accelerators, Novosibirsk 1986; Nauka v. 2, p. 72, 1987
4. G.L. Kotkin, S.I. Polityko, A. Schiller, V.G. Serbo: Z. Phys. C – Particles and Fields 39 (1988) 61
5. K.J.F. Gaemers, M. van der Horst: Nucl. Phys. B316 (1989) 269
6. D.Yu. Bardin et al.: Z. Phys. C – Particles and Fields 42 (1989) 679; Z. Phys. C – Particles and Fields 44 (1989) 149
7. A.A. Akhundov et al.: Z. Phys. C – Particles and Fields 45 (1990) 645
8. J.J Aubert et al.: Z. Phys. C – Particles and Fields 22 (1984) 341
9. S.V. Levonian et al.: H1-TR113, October 13 (1987)
10. F.W. Brasse et al.: Nucl. Phys. B110 (1976) 413
11. S. Stein et al.: Phys. Rev. D12 (1975) 1884
12. A.A Akhundov, D.Yu. Bardin, N.M. Schumeiko: Sov. J. Nucl. Phys. 26 (1977) 660
13. D.W. Duke, J.F. Owens: Phys. Rev. D30 (1984) 49
14. N.Yu. Volkonsky, L.V. Prokhorov: JETPH Lett. 21 (1975) 389